Sensors and Actuators A 257 (2017) 8–14

Contents lists available at ScienceDirect

Sensors and Actuators A: Physical

journal homepage: www.elsevier.com/locate/sna

Research Paper

Design on-chip width-modulated line-defect cavity array structure for multiplexing complex refractive index sensing

Fujun Sun, Jian Zhou, Lijun Huang, Zhongyuan Fu, Zhaoxiang Ding, Huiping Tian *

State Key Laboratory of Information Photonics and Optical Communications, School of Information and Communication Engineering, Beijing University of Posts and Telecommunications, Beijing 100876, China

ARTICLE INFO

Article history:
Received 18 July 2016
Received in revised form 4 January 2017
Accepted 30 January 2017
Available online 1 February 2017

Keywords:
Photonic crystal
Width-modulated line-defect micro-cavity
Complex refractive index sensing
Sensor array

ABSTRACT

We propose an integrated sensor array based on photonic crystal width-modulated line-defect micro-cavity for complex refractive index sensing. The width-modulated line-defect cavity is formed by decreasing the width of W1 waveguide with several holes in the first row shifted towards the line defect. By applying the three-dimensional finite-difference time-domain (3D-FDTD) simulation method, we demonstrate that simply shifting eight holes on each side by a distance of 100 nm is sufficient to achieve a high quality (Q) factor over 2×10^4. The proposed device consists of two cascaded micro-cavities with Q-factor over 1.5×10^4. The sensitivities of the real part (n) for cavity-1 and cavity-2 are 174.1 nm/RIU (refractive index unit) and 167.6 nm/RIU, respectively. The sensitivities of the imaginary part (k) are 230 nm/RIU and 200 nm/RIU for cavity-1 and cavity-2, respectively. In addition, a phenomenon that the sensitivity of imaginary part is much higher for smaller k values is described and explained. To the best of our knowledge, this is the first geometry to realize high-sensitivity multiplexing complex refractive index sensing.

1. Introduction

In the past few decades, numerous different integrated optical devices have been developed for refractive index sensing such as ring resonators [1,2], surface plasmon resonance [3,4], wire waveguides [5] and photonic crystal (PC) micro-cavities [6–23]. A key performance indicator of these sensors is the ability to detect the small change of refractive index (RI). For resonant sensors, this ability is expressed in terms of quality (Q) factor and sensitivity (S). Of all the different sensor architectures that have been developed, the sensors based on PC micro-cavities have attracted significant interests due to their compact size, high Q-factor [17–23] and high S [17–21]. The Q-factor describes the sharpness of the resonance. It represents the strength of light confined in a cavity and is defined as $Q = \lambda_0/\delta\lambda$, where λ_0 is resonance wavelength and $\delta\lambda$ is line-width of the resonance peak. The sensitivity of a device is reflected by the magnitude of light-matter interaction. In previous studies [6–20], PC sensors were all based on the detection of the real part of the RI. The sensitivity is expressed as $S_n = \Delta\lambda/\Delta n$, where $\Delta\lambda$ is the resonance wavelength shift and Δn is the real part of RI change. However, recently, Zhang et al. [12] proposed a complex refractive index sensing method that combined the detection of both real part (n) and imaginary part (k) of RI. The complex refractive index sensing method has the capability of ternary mixture concentration detection. The sensitivity of imaginary part of RI is given by $S_k = \Delta|\delta\lambda|/\Delta k$, where $\Delta|\delta\lambda|$ is the change of the mode line-width and Δk is the change of imaginary part.

In order to detect different analytes simultaneously on a single platform, PC sensor array always plays a significant role. Yang et al . [13] theoretically proposed a nanoscale PC sensor array on monolithic substrates using side-coupled resonant cavity array with the sensitivity of 130 nm/RIU and a Q-factor of around 3000. Liu et al. [14] theoretically studied a radius-graded PC sensor arrays with sensitivity up to 150 nm/RIU and Q-factor nearly 2000. Huang et al. [15] theoretically investigated a ring-slot array structure with Q-factors over 10^4 and sensitivities about 140 nm/RIU. Yan et al . [16] experimentally demonstrated a 2-channel L55 (55 represents the number of missing holes in Γ-K direction) PC bio-sensor array with sensitivity of 62 nm/RIU. Apparently, the sensor array mentioned above was only researched for real part of RI sensing, while multiplexing complex RI sensing has not been studied. However, the sensor in Ref. [12] only realized single point complex RI sensing. In addition, the sensitivities for n and k of the complex RI were 58 and 139 nm/RIU, respectively, which were relatively low.

In order to achieve multiplexing high-sensitivity complex RI sensing, an integrated sensor array based on photonic crystal

* Corresponding author.
E-mail address: hptian@bupt.edu.cn (H. Tian).

http://dx.doi.org/10.1016/j.sna.2017.01.024
0924-4247/

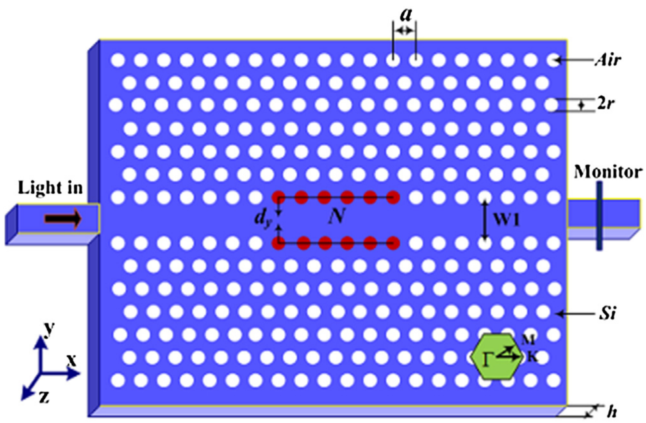

Fig. 1. Design of a width-modulated line-defect cavity based on W1 waveguide. The displacement of the holes (red air holes) relative to the unmodified lattice is given by d_y. N represents the number of shifting holes in the first row. (For interpretation of the references to colour in this figure legend, the reader is referred to the web version of this article.)

width-modulated line-defect micro-cavity (WMLDC) is proposed. The cavity is formed by locally modifying the position of a few of holes in the first row, nearest to the waveguide. By using 3D-FDTD simulation method, the number and distance of the shifting holes are adjusted to achieve high Q-factor. Based on the optimized results, two series-connected cavities are designed with Q-factors over 15,000. In addition, the sensitivities of the real part for cavity-1 and cavity-2 are 174.1 nm/RIU and 167.6 nm/RIU, respectively. As to the imaginary part, the sensitivities are 230 nm/RIU and 200 nm/RIU, respectively. Compared with Ref. [12], the calculated sensitivities are greatly improved. In addition, the results of simulation show that it has higher sensitivity for low k of RI.

2. Design of width-modulated line-defect PC micro-cavity

In this section, the design of PC WMLDC is demonstrated. The schematic of the proposed cavity is shown in Fig. 1. The cavity is based on a W1 (width of $3a$) photonic crystal waveguide (PCW) with a lattice period a of 480 nm. Triangular lattice air-holes are etched on a silicon slab (n = 3.48) with a thickness h = 220 nm. The holes radius r equals to 0.32a. N represents the number of shifting holes in the first row above and below the line-defect. The displacement of the holes (red air holes) shown in Fig. 1 is given by d_y. The light source is set at the input of W1 waveguide and monitor is located at the end of output W1 waveguide.

The dispersion curves of W1 PCW (d_y = 0 nm) and width-reduced (d_y = 100 nm) PCW obtained in TE-like polarization are shown in Fig. 2(a). The simulation results are calculated by the three-dimensional plane wave expansion (PWE) method. Due to the decreasing effective refractive index in the waveguide region, the dispersion curve of the width-reduced waveguide shifts to a higher frequency. As shown in Fig. 2(a), the guide band of width-reduced waveguide is located within the transmission window of W1 waveguide, thus the effective working wavelength of our proposed structure is confined in the range of width-reduced waveguide. The corresponding transmission spectra for W1 PCW and WMLDC PCW with N = 6, d_y = 100 nm are shown in Fig. 2(b), which are in agreement with the dispersion curves in Fig. 2(a). Analogous to L-type resonator cavity [9,10,16,17], light corresponding to the resonant wavelength is strongly localized in the defect area. This results in a dip in output spectrum of the waveguide and the corresponding electric field distribution of this cavity mode is shown in Fig. 2(b). As obviously seen in the inset of Fig. 2(b), there is a significant light amplification within the resonator. The strong optical field localization indicates the resonator should be very sensitive to the change of refractive index within these functionalized holes.

3. Optimization of number of shifting holes *N* and shifting distance d_y

Here we improve the Q-factor of our device by adjusting the number of shifting holes N and the shifting distance d_y. We study and optimize the proposed structure design by using commercial three dimensional finite difference time domain (3D-FDTD) software (FDTD Solutions, Lumerical). The 3D simulation domains are set as 12.5 μm × 9 μm × 2.2 μm. A perfectly matched layer (PML) is used as boundary condition to absorb the outgoing fields, and symmetries conditions have been exploited to save the simulation time. The number of layers of the stretched coordinate PML is 8. The auto non-uniform meshes are applied, which enable automatically to match the periodicity of the physical structure. In order to improve accuracy in the simulation, the mesh accuracy is chosen as 4, that is, the smallest mesh spacing is about 20 nm. TE-mode source and power monitor are placed at the input and output waveguide, respectively.

3.1. Number of shifting holes N

Fig. 3(a) shows drop transmission of the resonance for PC WMLDC with N = 4, 5, 6, 7 and 8 when d_y = 100 nm and the corresponding steady state electric field distribution is shown in Fig. 3(b). Fig. 3(c) shows the tendency of Q-factor and the resonance wavelength as a function of the number of shifting holes N. With the increase of N, the resonant wavelength shows a red shift. This is due to the increase in high-dielectric material in the cavity region. In addition, the Q-factor also increases monotonically with N, but it saturates as N tends to be larger. When N = 8, the Q-factor reaches 20,357. In order to design sensor array, the different micro-cavities should have independent separated resonant modes and large free spectral range (FSR). However, as shown in the inset of Fig. 3(a), the FSR of the two resonant modes decreases with the increase of N. Considering the larger FSR and higher Q-factor of the cavity, the number of shifting holes N = 6 is chosen as the optimized value.

3.2. Distance of shifting holes d_y

Fig. 4(a) shows the dip transmission spectra with the shift distance d_y varying from 75 nm to 125 nm when the number of shifting holes N = 6. The theoretical calculations for the resonance wavelength and Q-factor as a function of d_y are shown in Fig. 4(b). Owing to increasing high-dielectric material in the cavity region, the transmission dip shifts towards longer wavelength as the shifting distance increases. An optimal Q-factor of 15817 is observed when d_y = 100 nm.

4. PC width-modulated line-defect cavity sensors array design and sensitivity analysis

4.1. Sensing array design

Based on the optimized design of PC WMLDC, we demonstrate a photonic crystal sensor array with different shifting distance d_y but keeping shifting number fixed N = 6. As shown in Fig. 5(a), the specific parameters of the photonic crystal sensor array are as follows: cavity-1: d_y = 95 nm; cavity-2: d_y = 100 nm.

The transmission spectrum of the sensor array is shown in Fig. 5(b). As shown in Fig. 5(b), there exists two resonant dips in the transmission spectrum, and the corresponding resonant wavelengths are 1414.75 nm and 1423.07 nm, respectively. The